

Establishment and characterization of a novel murine model of pancreatic cancer cachexia

Katherine A. Michaelis¹ , Xinxia Zhu^{2†}, Kevin G. Burfeind^{1†}, Stephanie M. Krasnow², Peter R. Levasseur², Terry K. Morgan³ & Daniel L. Marks^{2*}

¹Medical Scientist Training Program, Oregon Health and Science University, Portland, USA; ²Papé Family Pediatric Research Institute, Oregon Health and Science University, Portland, USA; ³Departments of Pathology and Obstetrics and Gynecology, Oregon Health and Science University, Portland, USA

Abstract

Background Cachexia is a complex metabolic and behavioural syndrome lacking effective therapies. Pancreatic ductal adenocarcinoma (PDAC) is one of the most important conditions associated with cachexia, with >80% of PDAC patients suffering from the condition. To establish the cardinal features of a murine model of PDAC-associated cachexia, we characterized the effects of implanting a pancreatic tumour cell line from a syngeneic C57BL/6 KRAS^{G12D} P53^{R172H} Pdx-Cre^{+/+} (KPC) mouse.

Methods Male and female C57BL/6 mice were inoculated subcutaneously, intraperitoneally, or orthotopically with KPC tumour cells. We performed rigorous phenotypic, metabolic, and behavioural analysis of animals over the course of tumour development.

Results All routes of administration produced rapidly growing tumours histologically consistent with moderate to poorly differentiated PDAC. The phenotype of this model was dependent on route of administration, with orthotopic and intraperitoneal implantation inducing more severe cachexia than subcutaneous implantation. KPC tumour growth decreased food intake, decreased adiposity and lean body mass, and decreased locomotor activity. Muscle catabolism was observed in both skeletal and cardiac muscles, but the dominant catabolic pathway differed between these tissues. The wasting syndrome in this model was accompanied by hypothalamic inflammation, progressively decreasing brown and white adipose tissue uncoupling protein 1 (*Ucp1*) expression, and increased peripheral inflammation. Haematological and endocrine abnormalities included neutrophil-dominant leukocytosis and anaemia, and decreased serum testosterone.

Conclusions Syngeneic KPC allografts are a robust model for studying cachexia, which recapitulate key features of the PDAC disease process and induce a wide array of cachexia manifestations. This model is therefore ideally suited for future studies exploring the physiological systems involved in cachexia and for preclinical studies of novel therapies.

Keywords Pancreatic cancer; Cachexia; Cachexia models; Systemic inflammation

Received: 28 February 2017; Revised: 22 May 2017; Accepted: 29 May 2017

*Correspondence to: Daniel L. Marks, Papé Family Pediatric Research Institute, Oregon Health and Science University, 3181 SW Sam Jackson Park Road, L 481, Portland, OR 97239, USA. Email: marksd@ohsu.edu

†These authors contributed equally to this work

Background

Among the direst complications of chronic disease, cachexia is a multisystemic syndrome involving metabolic derangements, lean mass catabolism, and behavioural changes including anorexia and fatigue.^{1,2} Cachexia's impact extends beyond its widespread harm to quality of life, and it is estimated to be the direct cause of death in 20–30% of all cancer patients.^{3,4} In addition, cachexia contributes to cancer-associated morbidity

by weakening patients to the point they cannot tolerate chemotherapy or surgery.^{5–7} Despite the widespread need for improved cachexia therapies, there remain very few treatments for this condition.^{8,9} To design a therapy that addresses the root causes and manifestations of cachexia, it will be necessary to expand upon understanding cachexia pathophysiology through preclinical modelling. Because cachexia is by definition linked to its underlying disease processes, we sought to create a model fulfilling three criteria: (i) the underlying disease process is

known to cause cachexia in humans; (ii) the disease process and resultant cachexia can be induced reproducibly and consistently in a model organism; and (iii) the model recapitulates a maximal number of the systems and processes implicated in cachexia.

With these criteria in mind, an ideal pathophysiological framework for cachexia research is pancreatic ductal adenocarcinoma (PDAC). Among all forms of malignancy, PDAC is among the most highly associated with cachexia, with an estimated 83% of patients suffering from the condition.^{10–12} Furthermore, up to 20% of cancer patients die directly from cachexia, and many more become unable to tolerate chemotherapy regimens or surgery specifically because of decreased performance status associated with cachexia.^{13–18} Murine cachexia research has historically focused on four models: Lewis lung carcinoma (LLC), C26 colorectal adenocarcinoma (C26), patient-derived tumour xenografts (PDX), and genetically engineered mouse models (GEMMs). While these models provided a majority of the current understanding of cachexia, recent studies have highlighted the need for expanding upon and rigorously characterizing experimental methods for studying cachexia. For these reasons, we aimed to generate and establish the cardinal features of a PDAC cell line-induced, syngeneic, immunocompetent murine cachexia model.

To examine PDAC cachexia, we selected a cell line isolated from the PDAC lesion of a C57BL/6 mouse genetically modified to produce oncogenic KRAS^{G12D} and the mutant P53^{R172H} allele under a pancreas-specific Pdx1-Cre driver (KPC).¹⁹ KPC is one of the best-established murine models of PDAC, recapitulating a common oncogenic mutation in PDAC combined with a common tumour suppressor mutation associated with progression from PanIN III lesions to fulminant PDAC.²⁰ Using this cell line as a syngeneic KPC allograft, we tested the effects of three different routes of administration: subcutaneous (SQ), intraperitoneal (IP), and orthotopic (OT) pancreatic implantation. Animals were assessed for changes in body composition such as lean mass loss, fat mass loss, muscular atrophy, and neuroendocrine disturbances. In addition, animals were monitored for behaviours including food intake and locomotor activity. Finally, site-specific manifestations of cachexia were assessed throughout a variety of tissues, including the central nervous system, fast-twitch and slow-twitch fibre-enriched skeletal muscle groups, heart, liver, brown (BAT) and white adipose tissue (WAT), and blood.

Methods

Animals

Male and female C57BL/6J mice were obtained from The Jackson Laboratory (cat. #000664) and maintained in standard housing at 26°C and 12 h light/12 h dark cycles. Animals

were provided with *ad libitum* access to water and food (Purina rodent diet 5001; Purina Mills, St. Louis, MO, USA). In the week prior to tumour implantation, animals were transitioned to individual housing to acclimate to experimental conditions. Animal food intake and body weight were monitored daily immediately prior to lights out. All studies were conducted according to the National Institutes of Health Guide for the Care and Use of Laboratory Animals and approved by the Institutional Animal Care and Use Committee of Oregon Health and Science University.

Cell lines and tissue culture

The original KPC model expresses knock-in pancreas specific conditional alleles KRAS^{G12D} and TP53^{R172H} via the Pdx1-Cre driver. This model recapitulates PDAC tumour progression but is in a mixed 129/SvJae/C57BL/6 background. Therefore, the original KPC mouse was backcrossed into a C57BL/6 background for nine generations and pancreatic tumours from these mice were harvested to produce primary epithelial KPC lines, which were kindly provided by Dr Elizabeth Jaffee for use in these studies.¹⁹ Cells were maintained in RPMI 1640 supplemented with 10% heat-inactivated fetal bovine serum, 1% minimum essential medium non-essential amino acids, 1 mM sodium pyruvate, and 50 U/mL penicillin/streptomycin (Gibco, Gaithersburg, MD, USA), with incubators maintained at 37°C and 5% CO₂.

Generation of PDAC models

C57BL/6 mice aged 7–12 weeks were inoculated subcutaneously, intraperitoneally, or orthotopically with an inoculum of 1 million to 5 million KPC tumour cells, while controls received heat-killed cells in the same volume. Subcutaneous implantation was performed with a 1 mL injection of cell suspension in phosphate buffered saline into the interscapular subcutaneous space under brief isoflurane anaesthesia. IP implantation was performed as a 1 mL injection of cell suspension into the right iliac region, under brief isoflurane anaesthesia. Orthotopic implantation was performed as previously described by injecting 3 million cells in 40 µL into the tail of the pancreas, as defined by the pancreatic tissue immediately adjacent to the lower pole of the spleen, also under isoflurane anaesthesia.²¹

Nuclear magnetic resonance imaging

Nuclear magnetic resonance (NMR) measurements were taken at the beginning of the study for covariate adaptive randomization of tumour and sham groups to ensure equally distributed weight and body composition. Upon development of cachexia, mice were euthanized and subjected to repeat

NMR body composition analysis. For serial measurements of adiposity, one cohort was subjected to NMR analysis at time points corresponding to no muscle catabolism, moderate muscle catabolism, and severe muscle catabolism (5d, 7d, and 10d) and at time of sacrifice (11d).

Body temperature and locomotor activity measurement

Body temperature and voluntary home cage locomotor activity were measured via MiniMitter tracking devices (MiniMitter, Bend, OR, USA). Mice were implanted 3 days prior to tumour implantation with MiniMitter transponders in the intrascapular subcutaneous space. Using these devices, body temperature and movement counts in x-axis, y-axis, and z-axis were recorded in 5 min intervals (Vital View; MiniMitter).

Tissue collection and histology

At onset of cachexia or at pre-designated time points, animals were deeply anaesthetised by ketamine cocktail. Formalin-fixed paraffin-embedded histological sections were stained for haematoxylin and eosin. A surgical pathologist blinded to KPC administration group then reviewed them (i.e. subcutaneous, orthotopic, and IP) and scored them as positive or negative for (i) ragged infiltration; (ii) desmoplastic stromal response; and (iii) host inflammatory response. Tumour, brain, gastrocnemius muscle, liver, blood, interscapular BAT, and gonadal WAT were harvested and stored in RNAlater (Ambion Inc., Austin, TX, USA).

Quantitative qRT-PCR

RNA was extracted and purified with RNeasy Mini kits (Qiagen Inc., Germantown, MD, USA) and then reverse-transcribed into cDNA with a High Capacity cDNA Reverse Transcription Kit (Applied Biosystems Inc, Foster City, CA, USA). qRT-PCR was performed using TaqMan reagents and primer probes (Applied Biosystems Inc, Foster City, CA, USA). Catabolism genes in muscle (muscle atrophy F-box, *Mafbx*; muscle ring finger 1, *Murf1*; forkhead box O1, *Foxo1*), autophagy genes in heart (BCL2 interacting protein 3, *Bnip3*; cathespin L1, *Ctsl1*; GABA type a receptor associated protein like, *Gabarapl*), inflammatory response genes in the brain (interleukin-1 beta, *Il-1 β* ; tumour necrosis factor α , *Tnfa*; interleukin 1 receptor type 1, *Il-1r1*; arginase 1, *Arg1*; nitric oxide synthase 2, *Nos2*; P-selectin, *Selp*; interleukin-6, *Il-6*; leukaemia inhibitory factor, *Lif*), inflammatory response genes in liver (amyloid P component, serum, *Apcs*; orosomucoid 1, *Orm1*, *Il-1 β*), and thermogenic and inflammatory genes in WAT and BAT (uncoupling protein 1, *Ucp1*; interleukin 4, *Il-*

4, *Arg1*) were compared between tumour-bearing mice and tumour naïve controls by qRT-PCR and normalized to tissue-appropriate control genes (18S or beta actin).

Clinical assays

Whole blood counts with white blood cell differential were performed on EDTA-decoagulated samples obtained by cardiac puncture at time of necropsy using HemaVet 950 (Drew Scientific). Serum hormone assays were performed by the University of Virginia Ligand Assay and Analysis Core (URL: <https://med.virginia.edu/research-in-reproduction/ligand-assay-analysis-core/>). Testosterone was assayed in duplicate using IBL Mouse and Rat Testosterone Kit (catalogue IB79174, range 10.0–1600 ng/dL, and sensitivity 10 ng/dL). Blood glucose was measured immediately prior to euthanasia with electronic glucometer (OneTouch Ultra).

Statistical analysis

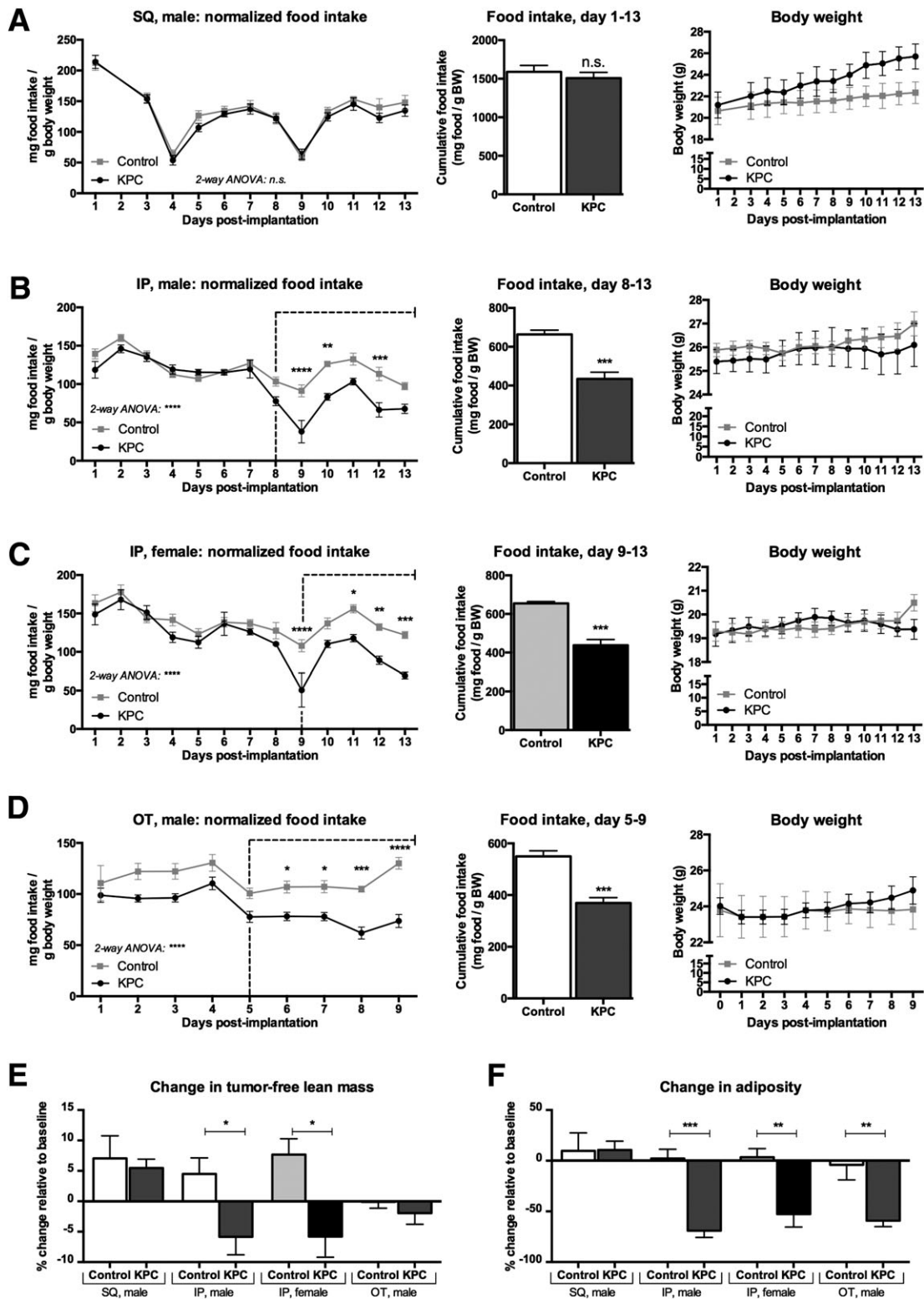
All reported studies are representative of three or more independent experiments, each with a minimum sample size of four per group. For comparison between tumour and control groups, data were assessed by Student's *t*-test or analysis of variance (Prism 6.0; GraphPad Software). Longitudinal variables in each route of administration were binned into the categories of pre-cachexia and cachexia on the basis of anorexia. Cachexia is here defined as the interval beginning with 2 consecutive days with an average food intake difference >10% and pre-cachexia as the interval between implantation and cachexia onset. Post hoc multiple comparisons tests were applied if a significant difference was present during the binned interval (pre-cachexia or cachexia). Bonferroni with baseline alpha 0.05 was used for multiple comparison tests to determine at which time points the KPC and control groups were significantly different.

Results

KPC allografts result in anorexia and body composition changes consistent with cachexia

KPC allografts lead to sickness behaviours, weight loss, and mortality, consistent with both PDAC and cachexia. The trajectory of illness follows a staged and reproducible series of manifestations, with onset of anorexia at 5–8 days and mortality at 11–14 days post-inoculation (Figure 1). All three routes of implantation resulted in rapid tumour growth without evidence of graft rejection. Despite being a robust route of administration for other models of cancer cachexia, subcutaneous implantation of KPC typically reaches tumour

Figure 1 Food intake, body weight, and body composition changes in KPC-induced cachexia. Dotted line demarcates cachexia stage as defined by continued presence of anorexia. Food intake throughout post-implantation phase, cumulative food intake during cachexia phase, and body weight over post-implantation phase in (A) subcutaneous, (B) intraperitoneal with male subjects, (C) intraperitoneal with female subjects, and (D) orthotopic routes of administration. Body composition changes were characterized with regard to lean mass (E) and adiposity (F). * $P < 0.05$; ** $P < 0.01$; *** $P < 0.001$; **** $P < 0.0001$.



burden end point (tumour volume in excess of 10% of body weight) prior to the onset of late-stage cachexia (Figure 1A). Although this was a consistent finding in younger animals, we did see an exception in an older female cohort, in which subcutaneous tumour implantation resulted in relative decreases in cumulative food intake in the final 7 days from 1454 ± 24 mg/g body weight in controls to 1011 ± 14 mg/g body weight in tumour-bearing animals ($P < 0.0001$, $n = 4$ per group). In this route of administration, tumour-bearing animals gained weight overall because of progressive increases in tumor mass ($F(1,60) = 67.15$, $P < 0.0001$, $n = 4$ per group) (Supporting Information, Figure 1). In contrast, IP tumour growth in males consistently resulted in anorexia within 8 days, with relative reductions in cumulative food intake over the final 6 days from 663.8 ± 21.8 mg/g body weight in controls to 434.0 ± 35.2 mg/g body weight in tumour-bearing animals ($P < 0.001$, $n = 4-5$ per group), despite unchanging total body weight (Figure 1B). In females, IP tumour growth resulted in anorexia within 9 days and reduced food intake over the final five days from 655.2 ± 9.2 mg/g body weight in controls to 437.4 ± 30.3 mg/g body weight in tumour-bearing animals ($P < 0.0001$, $n = 5$ per group), despite stable total body weight (Figure 1C). Similarly, orthotopic tumour growth resulted in a reduction in cumulative food intake over the final 5 days from 549.7 ± 21.3 mg/g body weight in controls to 369.4 ± 20.6 mg/g body weight in tumour-bearing animals ($P < 0.001$, $n = 5$ per group), without a change in total body weight (Figure 1D). The anorexia resulting from IP and orthotopic tumour implantation typically exceeds that seen in subcutaneous tumour implantation, in both time of onset and degree of severity.

Given that KPC-engrafted animals gain weight from tumour growth while losing weight from tissue catabolism, NMR body composition analysis was used to determine the degree of lean and adipose tissue loss. The tumour-free lean mass is defined as the lean mass measurement on NMR minus the tumour mass at necropsy, given that PDAC tumour volume is detected as lean mass on NMR. While control male mice gained $4.5 \pm 2.7\%$ lean mass over the course of 13 days, male mice implanted IP with KPC lost $5.9 \pm 3.0\%$ tumour-free lean mass ($P < 0.05$, $n = 4-5$ per group; Figure 1E). Similarly, control female mice gained $7.7 \pm 2.6\%$ lean mass over the course of 13 days, while female mice implanted IP with KPC lost $5.8 \pm 3.4\%$ tumour-free lean mass ($P < 0.05$, $n = 5$ per group; Figure 1E). In addition to lean mass wasting, KPC produces marked adipose tissue wasting. Control male mice gained $2.2 \pm 9.0\%$ fat mass over the course of 13 days, whereas male mice implanted IP with KPC lost $69.0 \pm 6.6\%$ fat mass ($P < 0.0001$, $n = 4-5$ per group; Figure 1F). Control female mice gained $3.5 \pm 8.4\%$ fat mass over the course of 13 days, while female mice implanted IP with KPC lost $52.6 \pm 12.8\%$ fat mass ($P < 0.01$, $n = 5$ per group; Figure 1F). Overall, wasting in the KPC model is observed in both lean and adipose tissue compartments and does not significantly differ between sexes.

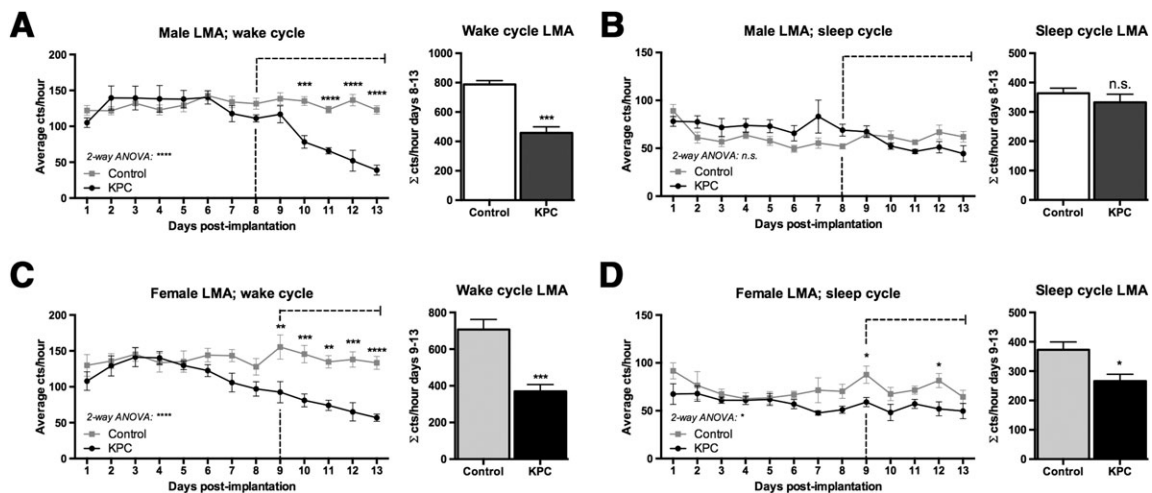
Decreased locomotor activity is an early and consistent feature of KPC-induced cachexia

Fatigue and lethargy are among the most significant and least therapeutically addressed manifestations of cachexia, and it is therefore important that cachexia models recapitulate these traits. In alignment with this aspect of cachexia in pancreatic cancer patients, decreased locomotor activity (LMA) is an early manifestation of KPC-induced cachexia. Analyses of LMA were subdivided into 12 h light and dark cycles, corresponding to sleep and wake cycles, respectively. In KPC-engrafted males, the cumulative sum of average wake cycle counts per hour during anorexia-defined cachexia decreased from 788 ± 26 to 458 ± 42 in tumour-bearing animals relative to controls ($P = 0.0002$, $n = 4-5$ per group; Figure 2A), with no changes in sleep cycle LMA. In KPC-engrafted females, the cumulative sum of average wake cycle counts per hour during anorexia-defined cachexia decreased from 707 ± 55 to 370 ± 37 in tumour-bearing animals relative to controls ($P = 0.001$, $n = 5$ per group; Figure 2C). In addition, KPC-engrafted females exhibited decreased LMA during sleep cycle, with a decrease from 373 ± 27 to 266 ± 23 in tumour-bearing animals relative to controls ($P = 0.02$, $n = 5$ per group; Figure 2D). The onset of activity loss is sexually dimorphic: females decrease LMA within 7–8 days of tumour growth, whereas males do not exhibit significant losses in LMA until 9–10 days of tumour growth. Furthermore, only females demonstrate a decrease in sleep cycle LMA. It is important to note that in females, a decrease in LMA is the first measurable behavioural change in KPC-induced cachexia and precedes anorexia by up to 2 days. In contrast, males demonstrate a simultaneous onset of anorexia and decreased LMA.

KPC allograft gross and microscopic features

The three routes of administration each resulted in distinct patterns of tumour growth, with particularly strong differences between the subcutaneous group vs. the IP and orthotopic groups. Subcutaneously implanted KPC cells formed only primary tumour masses isolated to the site of injection, with well-defined borders. Orthotopic KPC implants into the pancreas show ragged infiltration and patchy gross morphology. This type of IP transplantation did not lead to seeding of other peritoneal surfaces, or metastases to other organs. In contrast, IP implantation of KPC led to multifocal tumour growth on peritoneal surfaces, but with the majority of tumour growth localized to the pancreas. Haemorrhagic ascites were variably present in IP and orthotopic tumour models. Interestingly, tumour growth was sexually dimorphic, with males developing larger tumour masses than female animals (Supporting Information, Figure 2).

Figure 2 KPC engraftment progressively decreases locomotor activity in both sexes. Locomotor activity in average counts per hour, with cumulative sum of counts per hour during anorexia-defined cachexia stage. Dotted line demarcates the onset of anorexia. (A) Wake cycle locomotor activity in counts per hour in males and wake cycle cumulative counts per hour during anorexia stage, (B) sleep cycle locomotor activity in counts per hour in males and sleep cycle cumulative counts/hour during anorexia stage, (C) wake cycle locomotor activity in counts per hour in females and wake cycle cumulative counts/hour during anorexia stage, (D) sleep cycle locomotor activity in counts per hour in females and sleep cycle cumulative counts/hour during anorexia stage.



Histological sections strengthened these gross observations. The PDAC was moderate to poorly differentiated with conspicuous mitotic figures and coagulative tumour cell necrosis. In the subcutaneous allografts, tumour cells were arranged in nodules with well-circumscribed borders. There was minimal desmoplastic change to the stroma and no conspicuous host inflammatory response (Figure 3). In contrast, the orthotopic and IP allografts showed ragged tumour infiltration of the pancreas and a marked acute and chronic inflammatory host response. Because IP administration reliably induces pancreatic tumour growth without requiring surgery, we chose to further characterize the IP model using a systems-based approach.

Skeletal and cardiac muscle catabolism in KPC-engrafted animals proceeds through distinct mechanisms and are not sexually dimorphic

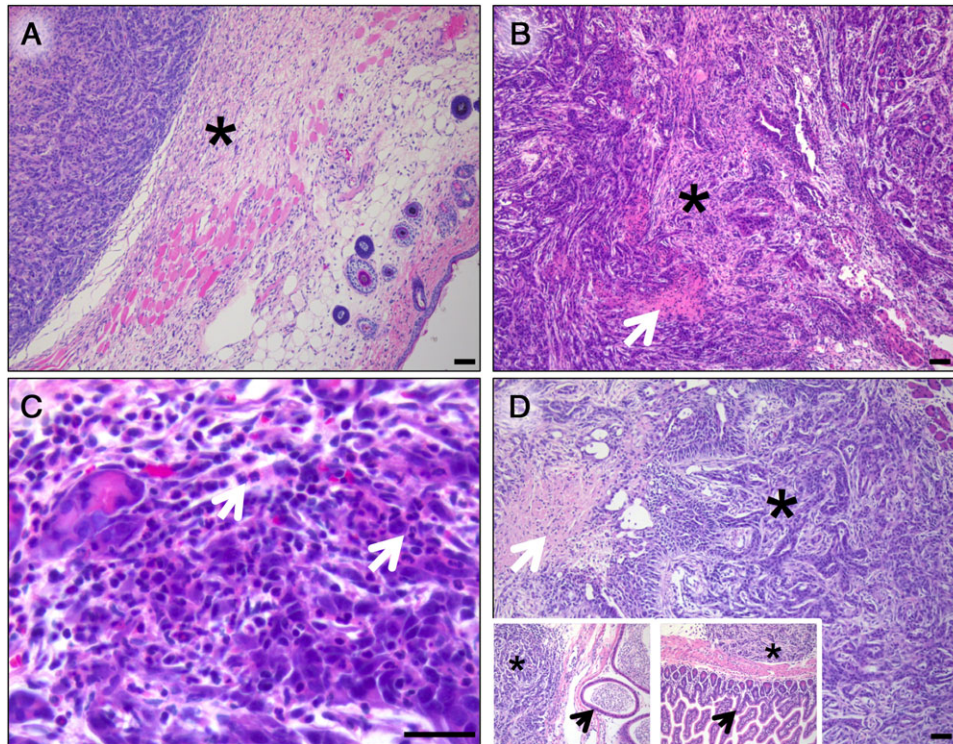
Two key subsets of muscle tissue, skeletal and cardiac, were examined in KPC-engrafted mice at end-stage cachexia. KPC tumour burden resulted in a progressive decrease in gastrocnemius weight, with no changes at day 5, a decrease from 5.23 ± 0.21 to 4.86 ± 0.13 mg/g initial body weight at day 7 ($P < 0.05$, $n = 5$ per group) and a further decrease from 5.09 ± 0.17 to 4.15 ± 0.22 mg/g initial body weight at day 10 ($P < 0.0001$, $n = 5$ per group) (Figure 4A). Late-stage KPC-engrafted animals demonstrated a decrease in heart weight from 126.7 ± 3.0 to 95.7 ± 5.1 mg in males ($P < 0.001$, $n = 4-5$ per group) and 96.9 ± 3.8 to 76.9 ± 2.1 mg in females ($P = 0.0019$, $n = 5$ per group) (Figure 4B). In addition, animals sacrificed in mid-stage cachexia 2 days following the onset of

anorexia demonstrate muscle loss in the fast-twitch fibre dominant muscles gastrocnemius, tibialis anterior, and quadriceps and, to a lesser extent, the slow-twitch fibre dominant muscle soleus (Figure 4C). Skeletal muscle catabolism was driven by a combination of E3 ubiquitin ligase induction and autophagy, both of which increased in a time-dependent manner (Figure 4D). By end stage, gastrocnemius catabolism in KPC-bearing animals vs. controls coincided with a 21.2 ± 3.4 -fold relative increase in gene expression of catabolic E3 ubiquitin ligase *Mafbx*, a 27.9 ± 9.2 -fold increase in *Murf1*, a 4.80 ± 0.85 -fold increase in *Foxo1*, a 5.39 ± 0.82 -fold increase in autophagy gene *Bnip3*, a 4.82 ± 0.72 -fold increase in *Ctsl*, a 7.8 ± 1.3 -fold increase in *Gabarapl*, and a 7.5 ± 1.9 -fold increase in adhesion molecule *Selp* ($P < 0.01$ for all, $n = 4$ per group) (Figure 4D). Cardiac atrophy in both sexes was accompanied by increased autophagy-related cardiac muscle gene expression of *Bnip3*, *Ctsl*, and *Gabarapl*, with relatively less induction of *Mafbx* and *Murf1* than skeletal muscle, and similar up-regulation of *Selp* (Figure 4E).²² Gene expression analysis comparing gastrocnemius, tibialis anterior, and quadriceps with soleus demonstrated relative sparing of slow-twitch muscle from activation of the ubiquitin proteasome and autophagy catabolic pathways during mid-stage KPC cachexia (Figure 4F).

KPC engraftment results in hypothalamic inflammation and activation of the hypothalamic-pituitary-adrenal axis

A large body of evidence demonstrates that the hypothalamus is a critical driver of cachexia, transducing

Figure 3 Histopathologic characteristics of KPC allografts. (A) Subcutaneous implantation of KPC allografts shows well-demarcated tumour nodule with minimal desmoplastic stroma (asterisk), no geographic necrosis, and no acute or chronic inflammation. (B) In contrast, orthotopic implantation into the pancreas leads to ragged infiltration of the organ with pronounced desmoplastic stroma, geographic necrosis (arrow), and acute inflammation (C). (D) Intraperitoneal implantation results in honing of tumour cells to the pancreas with similar histological findings to orthotopic implantation. However, IP administration also seeds multiple peritoneal sites [e.g. epididymis and small bowel (insets)]. Sections are stained with haematoxylin and eosin and photographed with $\times 10$ objective lens. Scale bar is 100 μm .

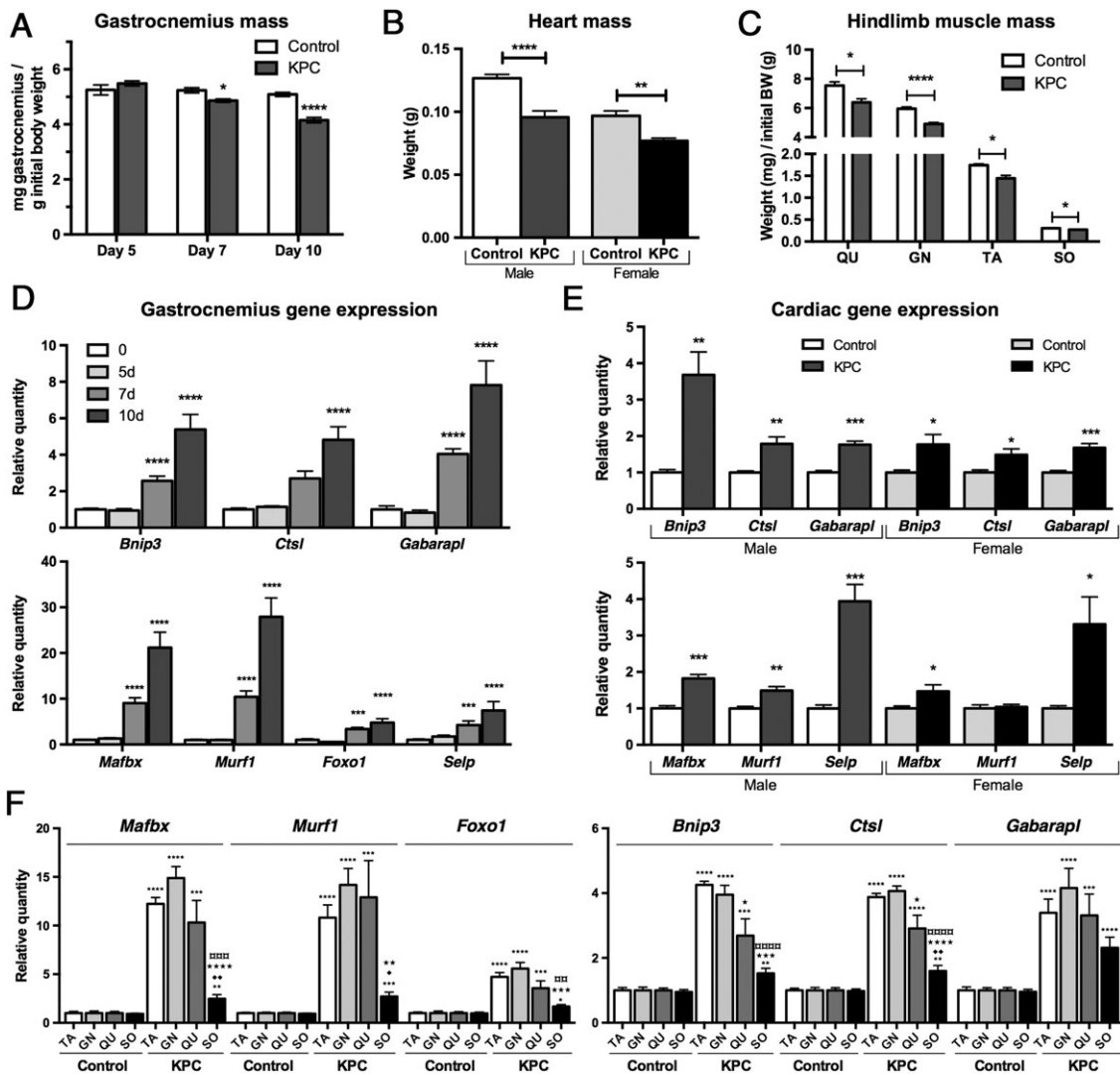


systemic inflammatory messages stemming from acute and chronic disease processes into a local and paracrine inflammatory response in the central nervous system.^{23–25} Consistent with this evidence, KPC induces an array of genes responsive to inflammatory stimuli in the hypothalamus. Compared with controls, tumour-engrafted animals demonstrated a 3.39 ± 0.66 -fold increase in *Il-1 β* ($P < 0.001$), a 4.5 ± 1.1 -fold increase in *Il-4* ($P < 0.01$), a 2.79 ± 0.11 -fold increase in *Il-1 α* ($P < 0.0001$), a 43.1 ± 7.6 -fold increase in *Selp* ($P < 0.001$), a 2.63 ± 0.16 -fold increase in *Arg1* ($P < 0.01$), and a 1.56 ± 0.17 -fold increase in *Nos2* ($P < 0.01$) ($n = 6$ per group) (Figure 5A). However, there were no differences in hypothalamic gene expression of the gp130 cytokines *Il-6* and *Lif*. The induction of inflammation is most pronounced in the hypothalamus and is not observed in other brain structures such as the cerebral cortex (Figure 5B). In alignment with previous findings that muscle atrophy during inflammatory stimuli is mediated by hypothalamic–pituitary–adrenal activation, end-stage KPC-engrafted animals demonstrate a 1.77 ± 0.19 -fold increase in hypothalamic expression of corticotropin-releasing hormone ($P < 0.05$) (Figure 5C).^{22,26}

KPC tumour progression induces loss of brown adipose tissue and white adipose tissue thermogenesis, accompanied by decreased core body temperature

An important mechanism seen in other subtypes of cancer cachexia, including LLC and C26 models, is energy loss through increased sympathetic nervous system outflow. In KPC-engrafted animals, core body temperature remained relatively constant until end-stage cachexia, with both light and dark cycle body temperature declining significantly in the last 2–3 days of illness (Figure 6A and B). End-stage cachexia was associated with severe depletion of BAT volume at necropsy (Supporting Information, Figure 3). Although BAT *Ucp1* expression did not differ significantly from controls at day 5, KPC-engrafted animals demonstrated a $52.27 \pm 10.69\%$ decrease at day 7 ($P < 0.05$, $n = 5$ per group) and an $88.19 \pm 0.03\%$ decrease at day 10 ($P < 0.0001$, $n = 5$ per group) (Figure 6C). Total adipose tissue in KPC-engrafted animals, however, underwent rapid loss over the course of the disease process, with significant changes detectable as early as 7 days ($P < 0.0001$, $n = 5$ –7 per group) (Figure 6D). WAT demonstrated

Figure 4 KPC engraftment results in catabolism and loss of skeletal and cardiac muscle. (A) Gastrocnemius mass in KPC and control animals sacrificed at designated time points. (B) Cardiac muscle at end-stage KPC cachexia in male and female animals. (C) Fast-twitch muscle groups gastrocnemius, tibialis anterior, quadriceps, and soleus weights in control and KPC-engrafted animals during mid-stage cachexia. (D–F) Autophagy, ubiquitin proteasome pathway, and inflammatory gene expression gastrocnemius (D), cardiac muscle (E), and representative fast-twitch and slow-twitch muscles of the hindlimb (F). * $P < 0.05$; ** $P < 0.01$; *** $P < 0.001$, **** $P < 0.0001$; asterisk, significantly different vs. matched muscle control; currency sign, significantly different vs. KPC tibialis anterior; black star, significantly different vs. KPC gastrocnemius; black diamond, significantly different vs. KPC quadriceps.



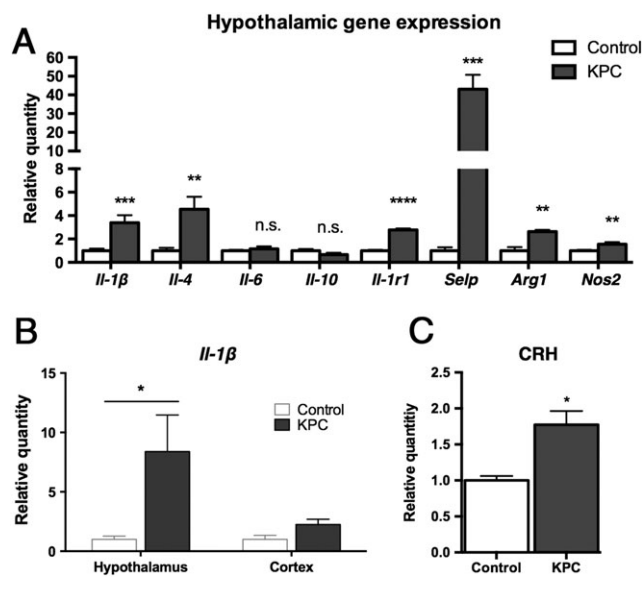
a $76.82 \pm 10.73\%$ decrease of *Ucp1* gene expression during end-stage illness ($P < 0.05$, $n = 6$ per group) (Figure 6E). Loss of *Ucp1* in WAT from KPC-engrafted animals was accompanied by an increase in markers of alternatively activated macrophage infiltration, with an 8.98 ± 2.27 -fold up-regulation of *Il-4* ($P < 0.01$, $n = 6$ per group) and a 25.24 ± 5.12 -fold up-regulation of *Arg1* ($P < 0.001$, $n = 6$ per group) (Figure 6F).

KPC allografts result in a systemic inflammatory response spanning multiple organ systems

The liver is extensively involved in systemic inflammatory responses to acute and chronic stimuli, contributing to

cachexia by producing pro-inflammatory signals and consuming amino acids for acute-phase protein synthesis. We specifically examined the acute-phase proteins pentraxin 2/APCS, which in mice serves an analogous role to C-reactive protein in humans, and *Orm1*, which has recently been shown to have anorexigenic properties.^{18,27,28} In males, KPC induced a 34.42 ± 6.89 -fold increase in *Apcs* ($P < 0.001$, $n = 4$ –5 per group) and a 6.61 ± 0.32 -fold increase in *Orm1* relative to controls ($P < 0.001$, $n = 4$ –5 per group) (Figure 7A). In females, KPC induced a 8.07 ± 0.87 -fold increase in *Apcs* ($P < 0.0001$, $n = 5$ per group) and a 5.30 ± 1.22 -fold increase in *Orm1* ($P < 0.01$, $n = 5$ per group) (Figure 7A). In addition to hepatic synthesis of acute-phase proteins, the pro-inflammatory

Figure 5 KPC induces hypothalamic inflammation and neuroendocrine alterations in the hypothalamic-pituitary-adrenal axis. (A) Hypothalamic gene expression in tumour vs. control, (B) comparison of hypothalamic and cortical *IL-1 β* gene expression, (C) hypothalamic *CRH* gene expression. * $P < 0.05$; ** $P < 0.01$; *** $P < 0.001$; **** $P < 0.0001$.



cytokine *IL-1 β* was induced 5.76 ± 0.63 -fold in KPC-engrafted males relative to controls ($P < 0.0001$, $n = 4$ – 5 per group) and 5.39 ± 0.77 -fold in KPC-engrafted females relative to controls ($P < 0.001$, $n = 5$ per group) (Figure 7B). The spleens of KPC mice demonstrated consistent enlargement at necropsy, with an average weight of 183 ± 22 mg in tumour-bearing mice vs. 70 ± 6 mg in controls ($P < 0.05$, $n = 5$ per group) (Figure 7C).

KPC allografts result in anaemia and neutrophil-dominant leukocytosis

One possible contributing mechanism of fatigue and cardiovascular strain in cancer cachexia is that chronic inflammation can result in anaemia of chronic disease via liver and bone marrow signalling.^{29,30} Consistent with a systemic inflammatory state, KPC tumour burden results in a marked neutrophil-dominant leukocytosis ($P < 0.001$) with increases in other innate immune cells including monocytes ($P < 0.01$) and eosinophils ($P < 0.01$) (Supporting Information, Figure 4A). Other haematological abnormalities included decreased haematocrit, erythrocytes, and platelets ($P < 0.05$). Although baseline haematological parameters were different between male and female animals, the observed anaemia and leukocytosis in KPC-engrafted animals of both sexes were indistinguishable. (Supporting Information, Figure 4B).

KPC-induced cachexia is associated with severe loss of circulating testosterone, without other detectable endocrine changes

Cancer cachexia is associated with neuroendocrine dysregulation, particularly in the hypothalamic-pituitary-adrenal and hypothalamic-pituitary-gonadal axes.^{22,31,32} KPC-engrafted males demonstrated marked hypogonadism, with a loss of >97% of free testosterone relative to controls at time of sacrifice ($P < 0.01$) (Figure 8A). While KPC-engrafted females also demonstrated slight decreases in serum-free testosterone, this difference did not reach statistical significance ($P = 0.13$). Unlike testosterone, accurate assessment of serum estradiol concentrations requires simultaneous cycling of female animals, which was not implemented in this study. Importantly, blood glucose concentrations at time of sacrifice were not elevated in KPC-engrafted mice, demonstrating that tumour growth did not result in diminished insulin secretion or diabetes as a mechanism of wasting (Figure 8B).

Discussion

A key rationale for characterization of the murine KPC model in the context of cachexia is that PDAC is one of the most cachexia-associated forms of cancer, with >80% of patients afflicted over the course of their illness. PDAC is also among the deadliest forms of cancer, with a 93% mortality rate in 5 years following diagnosis.^{33–36} Current approaches to treating PDAC include cytotoxic chemotherapy, ionizing radiation, and surgical resection.^{37,38} One possible reason these therapies are unsuccessful in achieving long-term survival is that they fail to treat cachexia, which is a key underlying cause of PDAC morbidity and mortality.^{10–12,39} Even PDAC tumours of exceptionally small size are capable of inducing the widespread physiologic, metabolic, and behavioural changes that define cachexia.^{6,33,40} Therefore, PDAC is a critical priority in cachexia research, and more effort must be directed toward elucidating molecular mechanisms and therapeutic targets in PDAC cachexia. Here, we demonstrate that syngeneic KPC allografts recapitulate key features of PDAC and induce a wide array of cachexia manifestations, including anorexia, decreased LMA, skeletal and cardiac muscle wasting, hypothalamic inflammation, and systemic inflammatory responses involving haematological and endocrine perturbations. Overall, this is an accurate and reproducible model of PDAC-induced cachexia and provides significant strengths relative to existing models.

In alignment with other cachexia models, we demonstrate muscle catabolism is a key aspect of KPC cachexia. Muscles with a high preponderance of fast-twitch fibres, that is, gastrocnemius, tibialis anterior, and quadriceps, were selected for skeletal muscle analysis because they are particularly susceptible to wasting in inflammatory states.²⁶

Figure 6 Body temperature decreases in conjunction with black adipose tissue and white adipose tissue UCP1 expression during KPC tumour progression, in conjunction with M2 macrophage activation in white adipose tissue. (A) Core body temperature in wake and sleep cycles in KPC vs. control males, (B) core body temperature in wake and sleep cycles in KPC vs. control females, (C) black adipose tissue gene expression of *Ucp1* at 5, 7, and 10 days of KPC tumour progression relative to control, (D) longitudinal assessment of body fat mass by nuclear magnetic resonance imaging over the course of 0–11 days in KPC vs. control animals, (E) white adipose tissue *Ucp1* expression at 10 days of KPC tumour progression vs. control. (F) White adipose tissue *Arg1* and *Il-4* expression at 10 days in KPC vs. control. **P* < 0.05; ***P* < 0.01; ****P* < 0.001; *****P* < 0.0001.

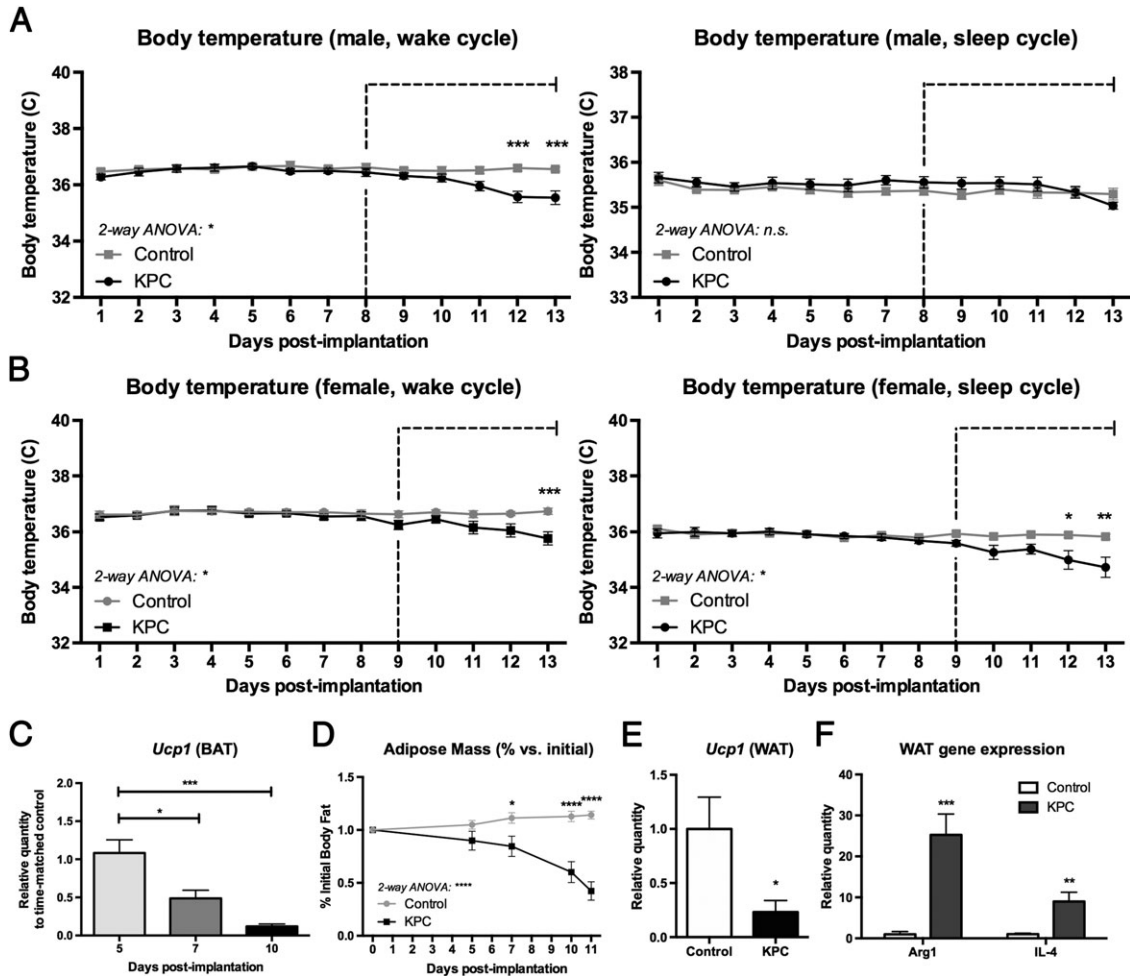
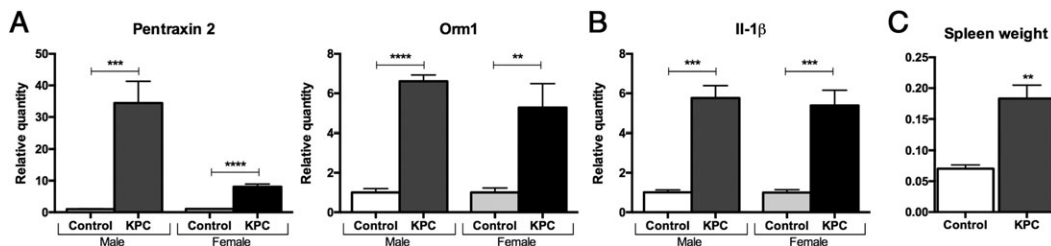


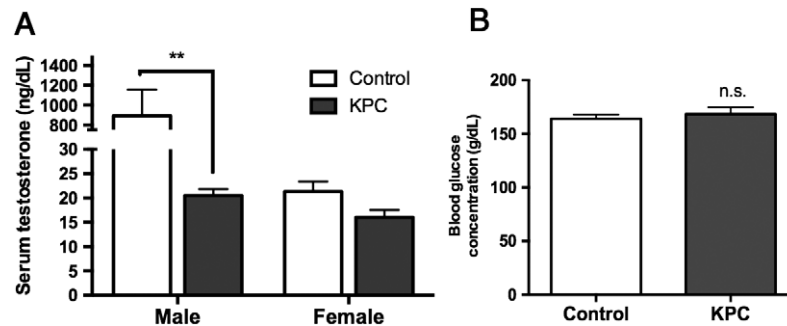
Figure 7 KPC tumour progression results in systemic inflammatory responses in hepatic tissue and spleen. (A) Relative hepatic gene expression of acute phase proteins pentraxin 2 (*Apcs*) and *Orm1* in control and KPC males and females (B) relative hepatic gene expression of *Il-1β* in KPC males and females, and (C) spleen weight at necropsy in KPC vs. control. **P* < 0.05; ***P* < 0.01; ****P* < 0.001; *****P* < 0.0001.



Indeed, KPC tumour growth induced tissue atrophy in all three of these muscle groups, corresponding to high expression levels of the ubiquitin ligases MAFBx and MuRF1 and their transcriptional inducer FOXO1. While there was

also a minor decrease in the mass of soleus, a muscle enriched with type I slow-twitch fibres, the atrophy was of a lesser magnitude and corresponded to a blunted induction of catabolic gene programming relative to fast-twitch

Figure 8 KPC tumour progression results in hypogonadism as manifested by decreased testosterone, without other endocrine changes including diabetes. (A) Serum-free testosterone in male and female KPC animals relative to control and (B) blood glucose concentration at time of sacrifice in KPC and control. ****** $P < 0.01$.



enriched muscles. Furthermore, the adhesion molecule P-selectin (SELP) was up-regulated in fast-twitch skeletal muscle, consistent with previous findings in rats bearing 3-methylcholanthrene (MCA) sarcoma.⁴¹ We also found an increase in the expression of autophagy genes in skeletal muscle, corroborating previous clinical evidence that this pathway of catabolism is a key contributor to lean tissue loss.⁴² In addition to skeletal muscle, cardiac muscle is often profoundly catabolic and functionally compromised by cancer cachexia.^{43–45} Cardiac dysfunction is independently associated with substantial morbidity and mortality in cachexia, and its mechanistic underpinnings are therefore an important topic of investigation. Cardiac muscle catabolism in cachexia has previously been linked to induction of autophagy and variably to expression of atrophy-associated ubiquitin ligases.^{46,47} Our data establish that the KPC model is similar to other cachexia models by producing skeletal muscle catabolism by E3 ubiquitin ligase activation and cardiac muscle catabolism via autophagy, but that both pathways are active in both tissue subsets. The importance of autophagy to both skeletal and cardiac muscle in this model is in alignment with recent work demonstrating that megestrol acetate ameliorates lean mass loss in skeletal and cardiac muscle via inhibition of autophagy.⁴⁸

In addition to muscle wasting, these data establish that KPC is a highly inflammatory disease state spanning multiple systems. One key site of inflammation in this model is the liver. Our data demonstrate a robust and sexually dimorphic up-regulation of pentraxin 2/APCS, the functional murine equivalent of C-reactive protein in human. C-reactive protein and APCS are induced in response to a variety of inflammatory stimuli primarily via IL-6, serving a key role in acute-phase responses.^{27,28} We also found that KPC increases hepatic expression of *Orm1*, another key acute-phase reactant in both mouse and human known to serve numerous important roles in energy balance, immunity, and capillary barrier modulation. Furthermore, *ORM1* is of metabolic and behavioural importance because it induces anorexia via leptin receptor signalling in the arcuate nucleus

of the hypothalamus.¹⁸ In mice, *ORM1* is primarily synthesized by the liver and is the only *ORM* isoform induced in response to inflammatory stimuli. The induction of both *Apcs* and *Orm1* indicates that KPC tumours induce a systemic inflammatory response and production of anorexigenic signalling proteins. Finally, we show that hepatic IL-1 β is induced in both sexes during KPC tumour growth, thereby establishing that the liver is a key site of multimodal inflammatory signalling in this model. Interestingly, we observed an up-regulation of SELP in functionally diverse tissues throughout the body, ranging from cardiac and skeletal muscle to the hypothalamus. This provides further mechanistic support to previous evidence that SELP polymorphisms are correlated with cachexia phenotype in clinical populations.^{41,49}

One key way in which the KPC model differs from existing cachexia models is that it does not induce *Ucp1* gene expression in BAT or WAT. Many studies have examined the role of increased sympathetic outflow in cachexia as a means of energy loss. The relevance of this mechanism is underscored by the ameliorative effects on sarcopenia and cachexia observed with the anabolic catabolic transforming agent espidolol, which acts as a nonspecific beta-1 and beta-2 adrenergic receptor antagonist.^{50,51} Sympathetic outflow increases can manifest as 'browning' of WAT or an increase of BAT activity through increased expression of genes such as *Ucp1*.^{52,53} UCP1 acts as an uncoupler of mitochondrial electron transport, which shifts adipocyte metabolism to increase thermogenesis while decreasing ATP synthesis, thereby increasing energy expenditure and lipid mobilization. The energy loss is not accompanied by increased core body temperature, even in thermoneutral conditions.⁵² While we demonstrate a similar pattern to these prior experiments in regard to loss of body temperature in late-stage cachexia, we found a loss in *Ucp1* in all adipose tissue rather than an increase. This may reflect that browning is a very early manifestation in cachexia that does not persist through end-stage disease or that energy wasting via adipose tissue browning may not be a

contributing factor in all aetiologies of cachexia. The finding that the BAT was severely depleted at both mid-stage cachexia and late-stage cachexia in this model argues for the former explanation and suggests that sympathetic activation may occur early in the disease course. This model importantly demonstrates that loss of adipose tissue is an early and defining event in the progression of KPC cachexia, occurring simultaneously with or prior to muscle catabolism. This corroborates previous investigations in both patient populations and murine models demonstrating that altered fat metabolism is a widespread and potent contributor to cachexia pathophysiology.^{54,55}

While commonly used preclinical murine models of cachexia such as LLC, C26, PDX, and GEMMs are clearly useful, each has substantial weaknesses. For example, implantation of LLC cells into syngeneic C57BL/6 mice provides a useful model for cachexia in lung cancer patients. However, this cell line was first isolated in 1951, and its wide use and inherent genomic instability has produced many distinctly heterogeneous subclones. As a result, LLC subclones range from highly cachexigenic to virtually unable to produce cachexia and vary in the ability to induce WAT browning.^{53,56,57} While C26 is also a very robust model, it is strongly dependent on IL-6 and leukemia inhibitory factor (LIF) signalling in a mechanism that applies to some, but not all, cancer patients.^{58,59} Corroborating this mechanism, IL-6 blocking therapies demonstrated clinical utility in a case series of cancer patients with extraordinarily high IL-6 levels.^{60,61} However, given IL-6 is not elevated in all forms of cancer cachexia and therefore not a universal driver, other models are needed to investigate IL-6-independent mechanisms. Patient-derived tumour xenografts are useful for their ability to test unique tumour cases, as well as investigate correlations between patient phenotype and murine cachexia outcomes, but require immunosuppression and are likely to lose a substantial proportion of signalling events due to the lack of species protein homology. Finally, GEMMs are variable with their time to spontaneous tumour formation and often demonstrate metabolic and behavioural abnormalities as a result of their genetic background. Further information on these cachexia models and others not discussed here, including the rat models Yoshida ascites hepatoma (YAH-130) and Walker 256 carcinosarcoma (Walker 256) and the murine MAC 16 adenocarcinoma (MAC16), are detailed elsewhere in a recent review.⁶²

In addition to the tumour-specific issues discussed earlier, the development of reliable preclinical models of cachexia is further hampered by the lack of standardization of key experimental details and measured outcomes. Therefore, recent efforts have focused on establishing standardized protocols for use of preclinical cachexia models and the characterization of their phenotypes, including a particularly robust study describing use and analysis of the C26 model.⁶³ Such details as the initial inoculum cell counts, site of

implantation, and details of animal husbandry (e.g. diets, sex, and housing conditions) do not follow general consensus guidelines, but these details are nonetheless critical to interpreting experimental outcomes. For example, despite the common rodent laboratory housing temperature at ~21°C (room temperature), the thermoneutral zone of mice ranges from 26°C during the active phase to over 30°C during the resting phase.^{64,65} Housing in relatively cold environments, particularly when animals are individually housed (as is common for cachexia studies), leads to a variety of stress responses and overt changes in inflammation and immune function.⁶⁶ For example, mice demonstrate altered behavioural and immune responses to lipopolysaccharide and have altered tumour growth and anti-tumour immune responses when housed in sub-thermoneutral environments.^{67,68} For these reasons, the KPC model was characterized with cage temperatures measured at 26°C and with adequate materials (nestlets) for thermoregulation. This combination avoids heat stress during the active phase but facilitates normal immune function and minimizes stress.^{64–66} Other environmental considerations in this study included a week long period of adaptation to novel environments and single housing prior to study initiation, regular handling in advance of the study to reduce stress associated with investigator interactions, and multiple sources of enrichment known to reduce stress in lab animals (Enviro Dri, nestlets).⁶⁹ Environmental design shortcomings of this study included that animals were individually housed in order to obtain individual LMA and food intake readings, despite the preference of mice to be group-housed. However, group-housed animals implanted with KPC did not demonstrate significant difference in onset to cachexia compared with singly housed animals, making it likely that this stressor was at most a minor contributor to the observed disease process (data not shown).

Another relatively understudied aspect of cachexia is sexual dimorphism. Clinical observations demonstrate that males are more adversely affected by cachexia than females, especially with regard to body weight, muscle mass, and muscle strength. Importantly, the rate of muscle wasting and weight loss correspond to survival in cancer patients,^{70,71} and males experience an increased degree of catabolism and an increased mortality risk in many different subsets of cancer.^{72–74} In the C26 model of cancer cachexia, male mice experience greater body weight loss, loss of skeletal and cardiac muscle, and mortality than tumour-bearing females because of the protective effects of oestrogen receptor signalling.⁴⁶ Our model demonstrates for the first time that LMA changes are sexually dimorphic and in females are the first behavioural signal of cachexia onset. In contrast to other cachexia models including C26, KPC-engrafted female animals do not demonstrate protection against cardiac muscle wasting or autophagy, despite smaller overall tumour burden. Because estradiol is highly dynamic across the estrus cycle, and animals

in this study were not simultaneously cycled, it was not possible to accurately assess whether hypogonadism could explain the relative lack of protection from cachexia in female KPC animals. Additional work will be necessary to determine whether hypogonadism or alternative inflammatory signalling can explain the lack of protection from cardiac wasting in KPC-engrafted females compared with other cachexia models.

In sum, the syngeneic KPC graft model provides a platform for further in-depth investigations of cancer cachexia. Future experiments will be essential to examine these manifestations using a cancer cachexia staging approach, given that an ideal therapeutic for cancer cachexia will be administered alongside other disease interventions at an earlier stage of illness. A particularly useful framework for this is the International Consensus Criteria, such that the parameters described in this study will be examined during pre-cachexia, cachexia, and refractory cachexia stages.⁵ Finally, this model will be of benefit for preclinical drug testing for both cachexia and PDAC interventions. Overall, this model adds substantially to experimental approaches to cancer cachexia with a specific focus on PDAC and will serve as a valuable resource for a wide variety of basic and translational approaches in future studies.

Acknowledgements

We thank Dr Elizabeth Jaffee, of Johns Hopkins University, for kindly providing C57BL/6 KPC epithelial PDAC cells derived in her laboratory. We additionally thank Mason Norgard for his technical support with follow-up studies, including animal monitoring and gene expression profiling. The authors certify that they comply with the ethical guidelines for publishing in the *Journal of Cachexia, Sarcopenia and Muscle*: update 2015.⁷⁵ This work was supported by NCI R01 CA184324 to D.L.M and the Brenden-Colson Center for Pancreatic Care.

References

- Grossberg AJ, Scarlett JM, Marks DL. Hypothalamic mechanisms in cachexia. *Physiol Behav* 2010;**100**:478–489.
- Tisdale MJ. Biology of cachexia. *J Natl Cancer Inst* 1997;**89**:1763–1773.
- von Haehling S, Anker SD. Cachexia as a major underestimated and unmet medical need: facts and numbers. *J Cachexia Sarcopenia Muscle* 2010;**1**:1–5.
- von Haehling S, Anker MS, Anker SD. Prevalence and clinical impact of cachexia in chronic illness in Europe, USA, and Japan: facts and numbers update 2016. *J Cachexia Sarcopenia Muscle* 2016;**7**:507–509.
- Fearon K, Strasser F, Anker SD, Bosaeus I, Bruera E, Fainsinger RL, et al. Definition and classification of cancer cachexia: an international consensus. *Lancet Oncol* 2011;**12**:489–495.
- Fearon KC, Glass DJ, Guttridge DC. Cancer cachexia: mediators, signaling, and metabolic pathways. *Cell Metab* 2012;**16**:153–166.
- Tisdale MJ. Cachexia in cancer patients. *Nat Rev Cancer* 2002;**2**:862–871.
- Femia RA, Goyette RE. The science of megestrol acetate delivery: potential to improve outcomes in cachexia. *BioDrugs* 2005;**19**:179–187.
- Ruiz Garcia V, López-Briz E, Carbonell Sanchis R, Gonzalez Perales JL, Bort-Marti S. Megestrol acetate for treatment of anorexia–cachexia syndrome. *Cochrane Database Syst Rev* 2013;<https://doi.org/10.1002/14651858.CD004310.pub3>.
- Aoyagi T, Terracina KP, Raza A, Matsubara H, Takabe K. Cancer cachexia, mechanism and treatment. *World J Gastrointest Oncol* 2015;**7**:17–29.
- Fearon K, Arends J, Baracos V. Understanding the mechanisms and treatment options in cancer cachexia. *Nat Rev Clin Oncol* 2013;**10**:90–99.
- Mueller TC, Burmeister MA, Bachmann J, Martignoni ME. Cachexia and pancreatic cancer: are there treatment options? *World J Gastroenterol* 2014;**20**:9361–9373.
- Fearon KC, Voss AC, Hustead DS, Cancer Cachexia Study Group. Definition of cancer cachexia: effect of weight loss, reduced food intake, and systemic inflammation

Online supplementary material

Additional Supporting Information may be found online in the supporting information tab for this article.

Data S1. Supporting info item

Figure S1. Food intake and body weight changes in an older female cohort demonstrating subcutaneous KPC-induced cachexia. Dotted line demarcates cachexia stage as defined by continued presence of anorexia. Food intake throughout post-implantation phase, cumulative intake during cachexia phase, and body weight over post-implantation phase in subcutaneous routes of administration in a 4-month old female cohort. *, $P < 0.05$; **, $P < 0.01$; *** $P < 0.001$; ****, $P < 0.0001$.

Figure S2. Tumour burden at necropsy in male and female animals. Total tumour size at time of end-stage cachexia in males and females in the same experiment implanted with intraperitoneal KPC. *, $p < 0.05$

Figure S3. Gross appearance of BAT at necropsy. Representative photographs of interscapular brown adipose tissue in KPC-engrafted animals relative to controls. (a) Gross appearance of dorsum during end-stage cachexia; white arrow indicates BAT. (b) Resected interscapular brown adipose tissue.

Figure S4. KPC engraftment results in hematologic changes including anaemia and neutrophil-dominant leukocytosis. (a) Complete blood count with differential during end-stage cachexia in males with IP KPC vs. controls, and (b) complete blood count with differential during end-stage cachexia in males vs. females with IP KPC. *, $P < 0.05$; **, $P < 0.01$; *** $P < 0.001$.

Conflict of interest

None declared.

- on functional status and prognosis. *Am J Clin Nutr* 2006;**83**:1345–1350.
14. Prado CM, Baracos VE, McCargar LJ, Mourtzakis M, Mulder KE, Reiman T, et al. Body composition as an independent determinant of 5-fluorouracil-based chemotherapy toxicity. *Clin Cancer Res* 2007;**13**:3264–3268.
 15. Prado CM, Baracos VE, McCargar LJ, Reiman T, Mourtzakis M, Tonkin K, et al. Sarcopenia as a determinant of chemotherapy toxicity and time to tumor progression in metastatic breast cancer patients receiving capecitabine treatment. *Clin Cancer Res* 2009;**15**:2920–2926.
 16. Ross PJ, Ashley S, Norton A, Priest K, Waters JS, Eisen T, et al. Do patients with weight loss have a worse outcome when undergoing chemotherapy for lung cancers? *Br J Cancer* 2004;**90**:1905–1911.
 17. Stewart GD, Skipworth RJ, Fearon KC. Cancer cachexia and fatigue. *Clin Med (Lond)* 2006;**6**:140–143.
 18. Sun Y, Yang Y, Qin Z, Cai J, Guo X, Tang Y, et al. The acute-phase protein orosomucoid regulates food intake and energy homeostasis via leptin receptor signaling pathway. *Diabetes* 2016;**65**:1630–1641.
 19. Foley K, Rucki AA, Xiao Q, Zhou D, Leubner A, Mo G, et al. Semaphorin 3D autocrine signaling mediates the metastatic role of annexin A2 in pancreatic cancer. *Sci Signal* 2015;**8**:ra77.
 20. Guerra C, Barbacid M. Genetically engineered mouse models of pancreatic adenocarcinoma. *Mol Oncol* 2013;**7**:232–247.
 21. Chai MG, Kim-Fuchs C, Angst E, Sloan EK. Bioluminescent orthotopic model of pancreatic cancer progression. *J Vis Exp* 2013;**76**.
 22. Braun TP, Szumowski M, Levasseur PR, Grossberg AJ, Zhu X, Agarwal A, et al. Muscle atrophy in response to cytotoxic chemotherapy is dependent on intact glucocorticoid signaling in skeletal muscle. *PLoS One* 2014;**9**: p. e106489.
 23. Burfeind KG, Michaelis KA, Marks DL. The central role of hypothalamic inflammation in the acute illness response and cachexia. *Semin Cell Dev Biol* 2016;**54**:42–52.
 24. Ezeoke CC, Morley JE. Pathophysiology of anorexia in the cancer cachexia syndrome. *J Cachexia Sarcopenia Muscle* 2015;**6**:287–302.
 25. Mendes MC, Pimentel GD, Costa FO, Carvalheira JB. Molecular and neuroendocrine mechanisms of cancer cachexia. *J Endocrinol* 2015;**226**:R29–R43.
 26. Braun TP, Zhu X, Szumowski M, Scott GD, Grossberg AJ, Levasseur PR. Central nervous system inflammation induces muscle atrophy via activation of the hypothalamic–pituitary–adrenal axis. *J Exp Med* 2011;**208**:2449–2463.
 27. Ansar W, Ghosh S. C-reactive protein and the biology of disease. *Immunol Res* 2013;**56**:131–142.
 28. Pepys MB, Hirschfield GM. C-reactive protein: a critical update. *J Clin Invest* 2003;**111**:1805–1812.
 29. Maccio A, Madeddu C, Gramignano G, Mulas C, Tanca L, Cherchi MC, et al. The role of inflammation, iron, and nutritional status in cancer-related anemia: results of a large, prospective, observational study. *Haematologica* 2015;**100**:124–132.
 30. Theurl M, Nairz M, Schroll A, Sonnweber T, Asshoff M, Haschka D, et al. Hepcidin as a predictive factor and therapeutic target in erythropoiesis-stimulating agent treatment for anemia of chronic disease in rats. *Haematologica* 2014;**99**:1516–1524.
 31. Dev R. The assessment and management of cancer cachexia: hypogonadism and hypermetabolism among supportive and palliative care patients. *Curr Opin Support Palliat Care* 2014;**8**:279–285.
 32. Burney BO, Garcia JM. Hypogonadism in male cancer patients. *J Cachexia Sarcopenia Muscle* 2012;**3**:149–155.
 33. Bachmann J, Büchler MW, Friess H, Martignoni ME. Cachexia in patients with chronic pancreatitis and pancreatic cancer: impact on survival and outcome. *Nutr Cancer* 2013;**65**:827–833.
 34. Bachmann J, Heiligensetzer M, Krakowski-Roosen H, Büchler MW, Friess H, Martignoni ME. Cachexia worsens prognosis in patients with resectable pancreatic cancer. *J Gastrointest Surg* 2008;**12**:1193–1201.
 35. Bachmann J, Ketterer K, Marsch C, Fechtner K, Krakowski-Roosen H, Büchler MW, et al. Pancreatic cancer related cachexia: influence on metabolism and correlation to weight loss and pulmonary function. *BMC Cancer* 2009;**9**:255.
 36. Uomo G, Gallucci F, Rabitti PG. Anorexia–cachexia syndrome in pancreatic cancer: recent development in research and management. *JOP* 2006;**7**:157–162.
 37. Von Hoff DD, Ervin T, Arena FP, Chiorean EG, Infante J, Moore M, et al. Increased survival in pancreatic cancer with nab-paclitaxel plus gemcitabine. *N Engl J Med* 2013;**369**:1691–1703.
 38. Paulson AS, Tran Cao HS, Tempero MA, Lowy AM. Therapeutic advances in pancreatic cancer. *Gastroenterology* 2013;**144**:1316–1326.
 39. Del Fabbro E. Current and future care of patients with the cancer anorexia–cachexia syndrome. *Am Soc Clin Oncol Educ Book* 2015;**e229–e237**.
 40. Dewys WD, Begg C, Lavin PT, Band PR, Bennett JM, Bertino JR, et al. Prognostic effect of weight loss prior to chemotherapy in cancer patients. Eastern Cooperative Oncology Group. *Am J Med* 1980;**69**:491–497.
 41. Tan BH, Fladvad T, Braun TP, Vigano A, Strasser F, Deans DA, et al. P-selectin genotype is associated with the development of cancer cachexia. *EMBO Mol Med* 2012;**4**:462–471.
 42. Aversa Z, Pin F, Lucia S, Penna F, Verzaro R, Fazi M, et al. Autophagy is induced in the skeletal muscle of cachectic cancer patients. *Sci Rep* 2016;**6**:30340.
 43. Xu H, Crawford D, Hutchinson KR, Youtz DJ, Lucchesi PA, Velten M, et al. Myocardial dysfunction in an animal model of cancer cachexia. *Life Sci* 2011;**88**:406–410.
 44. Olivan M, Springer J, Busquets S, Tschirner A, Figueras M, Toledo M, et al. Theophylline is able to partially revert cachexia in tumour-bearing rats. *Nutr Metab (Lond)* 2012;**9**:76.
 45. Der-Torossian H, Gourin CG, Couch ME. Translational implications of novel findings in cancer cachexia: the use of metabolomics and the potential of cardiac malfunction. *Curr Opin Support Palliat Care* 2012;**6**:446–450.
 46. Cosper PF, Leinwand LA. Cancer causes cardiac atrophy and autophagy in a sexually dimorphic manner. *Cancer Res* 2011;**71**:1710–1720.
 47. Hinch EC, Sullivan-Gunn MJ, Vaughan VC, McGlynn MA, Lewandowski PA. Disruption of pro-oxidant and antioxidant systems with elevated expression of the ubiquitin proteasome system in the cachectic heart muscle of nude mice. *J Cachexia Sarcopenia Muscle* 2013;**4**:287–293.
 48. Musolino V, Palus S, Tschirner A, Drescher C, Gliozzi M, Carresi C, et al. Megestrol acetate improves cardiac function in a model of cancer cachexia-induced cardiomyopathy by autophagic modulation. *J Cachexia Sarcopenia Muscle* 2016;**7**:555–566.
 49. Avan A, Avan A, Le Large TYS, Mambrini A, Funel N, Maftouh M, et al. AKT1 and SELP polymorphisms predict the risk of developing cachexia in pancreatic cancer patients. *PLoS One* 2014;**9**: p. e108057.
 50. Potsch MS, Tschirner A, Palus S, von Haehling S, Doehner W, Beadle J, et al. The anabolic catabolic transforming agent (ACTA) espidolol increases muscle mass and decreases fat mass in old rats. *J Cachexia Sarcopenia Muscle* 2014;**5**:149–158.
 51. Stewart Coats AJ, Ho GF, Prabhaskar K, von Haehling S, Tilson J, Brown R, et al. Espidolol for the treatment and prevention of cachexia in patients with stage III/IV non-small cell lung cancer or colorectal cancer: a randomized, double-blind, placebo-controlled, international multicentre phase II study (the ACT-ONE trial). *J Cachexia Sarcopenia Muscle* 2016;**7**:355–365.
 52. Petruzzelli M, Schweiger M, Schreiber R, Campos-Olivas R, Tsoli M, Allen J, et al. A switch from white to brown fat increases energy expenditure in cancer-associated cachexia. *Cell Metab* 2014;**20**:433–447.
 53. Kir S, White JP, Kleiner S, Kazak L, Cohen P, Baracos VE, et al. Tumour-derived PTH-related protein triggers adipose tissue browning and cancer cachexia. *Nature* 2014;**513**:100–104.
 54. Argiles JM, Busquets S, Stemmler B, López-Soriano FJ. Cancer cachexia: understanding the molecular basis. *Nat Rev Cancer* 2014;**14**:754–762.
 55. Tanaka Y, Eda H, Tanaka T, Udagawa T, Ishikawa T, Horii I, et al. Experimental cancer cachexia induced by transplantable colon 26 adenocarcinoma in mice. *Cancer Res* 1990;**50**:2290–2295.

56. Simpson-Herren L, Sanford AH, Holmquist JP. Cell population kinetics of transplanted and metastatic Lewis lung carcinoma. *Cell Tissue Kinet* 1974;**7**:349–361.
57. van Lamsweerde AL, Henry N, Vaes G. Metastatic heterogeneity of cells from Lewis lung carcinoma. *Cancer Res* 1983;**43**:5314–5320.
58. Bonetto A, Aydogdu T, Jin X, Zhang Z, Zhan R, Puzis L, et al. JAK/STAT3 pathway inhibition blocks skeletal muscle wasting downstream of IL-6 and in experimental cancer cachexia. *Am J Physiol Endocrinol Metab* 2012;**303**:E410–E421.
59. Seto DN, Kandarian SC, Jackman RW. A key role for leukemia inhibitory factor in C26 cancer cachexia. *J Biol Chem* 2015;**290**:19976–19986.
60. Ando K, Takahashi F, Motojima S, Nakashima K, Kaneko N, Hoshi K, et al. Possible role for tocilizumab, an anti-interleukin-6 receptor antibody, in treating cancer cachexia. *J Clin Oncol* 2013;**31**:e69–e72.
61. Berti A, Boccalatte F, Sabbadini MG, Dagna L. Assessment of tocilizumab in the treatment of cancer cachexia. *J Clin Oncol* 2013;**31**:2970.
62. Ishida J, Saitoh M, Doehner W, von Haehling S, Anker M, Anker SD, et al. Animal models of cachexia and sarcopenia in chronic illness: cardiac function, body composition changes and therapeutic results. *Int J Cardiol* 2017;**238**:12–18.
63. Bonetto A, Rupert JE, Barreto R, Zimmers TA. The Colon-26 Carcinoma Tumor-bearing Mouse as a Model for the Study of Cancer Cachexia. *J Vis Exp* 2016;**117**:e54893.
64. Gaskill BN, Gordon CJ, Pajor EA, Lucas JR, Davis JK, Garner JP. Heat or insulation: behavioral titration of mouse preference for warmth or access to a nest. *PLoS One* 2012;**7**: p. e32799.
65. Gordon CJ. *Temperature Regulation in Laboratory Rodents*. Cambridge: Cambridge University Press; 1993.
66. Karp CL. Unstressing intemperate models: how cold stress undermines mouse modeling. *J Exp Med* 2012;**209**:1069–1074.
67. Rudaya AY, Steiner AA, Robbins JR, Dragic AS, Romanovsky AA. Thermoregulatory responses to lipopolysaccharide in the mouse: dependence on the dose and ambient temperature. *Am J Physiol Regul Integr Comp Physiol* 2005;**289**:R1244–R1252.
68. Kokolus KM, Capitano ML, Lee CT, Eng JW, Waight JD, Hylander BL, et al. Baseline tumor growth and immune control in laboratory mice are significantly influenced by subthermoneutral housing temperature. *Proc Natl Acad Sci U S A* 2013;**110**:20176–20181.
69. Gaskill BN, Karas AZ, Garner JP, Pritchett-Corning KR. Nest building as an indicator of health and welfare in laboratory mice. *J Vis Exp* 2013;**82**:51012.
70. Di Sebastiano KM, Yang L, Zbuk K, Wong RK, Chow T, Koff D, et al. Accelerated muscle and adipose tissue loss may predict survival in pancreatic cancer patients: the relationship with diabetes and anaemia. *Br J Nutr* 2013;**109**:302–312.
71. Donohoe CL, Ryan AM, Reynolds JV. Cancer cachexia: mechanisms and clinical implications. *Gastroenterol Res Pract* 2011;**2011**:601434.
72. Hendifar A, Yang D, Lenz F, Lurje G, Pohl A, Lenz C, et al. Gender disparities in metastatic colorectal cancer survival. *Clin Cancer Res* 2009;**15**:6391–6397.
73. Palomares MR, Sayre JW, Shekar KC, Lillington LM, Chlebowski RT. Gender influence on weight-loss pattern and survival of nonsmall cell lung carcinoma patients. *Cancer* 1996;**78**:2119–2126.
74. Baracos VE, Reiman T, Mourtzakis M, Gioulbasanis I, Antoun S. Body composition in patients with non-small cell lung cancer: a contemporary view of cancer cachexia with the use of computed tomography image analysis. *Am J Clin Nutr* 2010;**91**:1133S–1137S.
75. von Haehling S, Morley JE, Coats AJS, Anker SD. Ethical guidelines for publishing in the Journal of Cachexia, Sarcopenia and Muscle: update 2015. *J Cachexia Sarcopenia Muscle* 2015;**6**: 315–316.